

# NICS: The TNG Near Infrared Camera Spectrometer <sup>★</sup>

C. Baffa<sup>1</sup>, G. Comoretto<sup>1</sup>, S. Gennari<sup>1</sup>, F. Lisi<sup>1</sup>, E. Oliva<sup>1,4</sup>, V. Biliotti<sup>1</sup>, A. Checcucci<sup>1</sup>, V. Gavriushev<sup>2</sup>,  
E. Giani<sup>1</sup>, F. Ghinassi<sup>4</sup>, L.K. Hunt<sup>2</sup>, R. Maiolino<sup>1</sup>, F. Mannucci<sup>2</sup>, G. Marcucci<sup>3</sup>, M. Sozzi<sup>2</sup>, P. Stefanini<sup>1</sup>,  
and L. Testi<sup>1</sup>

<sup>1</sup> Osservatorio Astrofisico di Arcetri, Largo E. Fermi 5, Firenze, Italy

<sup>2</sup> Centro per l'Astronomia Infrarossa e lo Studio del Mezzo Interstellare-CNR, Largo E. Fermi 5, Firenze, Italy

<sup>3</sup> Dipartimento di Astronomia e Scienze dello Spazio, Università di Firenze, Largo E. Fermi 5, Firenze, Italy

<sup>4</sup> Centro Galileo Galilei, Santa Cruz De La Palma, TF, La Palma, Spain.

Received.....; Accepted.....

**Abstract.** NICS (acronym for Near Infrared Camera Spectrometer) is the near-infrared cooled camera-spectrometer that has been developed by the Arcetri Infrared Group at the Arcetri Astrophysical Observatory, in collaboration with the CAISMI-CNR for the TNG (the Italian National Telescope Galileo at La Palma, Canary Islands, Spain). As NICS is in its scientific commissioning phase, we report its observing capabilities in the near-infrared bands at the TNG, along with the measured performance and the limiting magnitudes. We also describe some technical details of the project, such as cryogenics, mechanics, and the system which executes data acquisition and control, along with the related software.

**Key words.** Instrumentation: spectrographs, Instrumentation: polarimeters, Near Infrared

## 1. Introduction

The 3.5m Italian National Telescope Galileo (TNG) (Barbieri 1995), under operation on La Palma (Canary Islands), included a general purpose near-infrared camera/spectrometer in its Instrument Plan for first-light operations (Fusi Pecci et al. 1992, Fusi Pecci et al. 1994). The telescope itself is not optimized for the thermal infrared bands, so NICS was designed to operate at near-infrared wavelengths, from 0.95  $\mu\text{m}$  up to 2.50  $\mu\text{m}$ , avoiding the spectral range where the ambient blackbody radiation could degrade the signal-to-noise ratio of the observations. Moreover, this spectral range is conveniently covered by HgCdTe (or MCT for Mercury-Cadmium-Telluride) large format focal-plane array detectors currently available, which, at present, offer the best combination of quality and low read-noise. NICS was the only infrared instrument for the first light of the TNG; as a consequence, we decided to incorporate a sufficient degree of operation flexibility by adopting a collimator/camera optical scheme along with a good pupil image where a number of analyzers (filters, grisms, polarizers) can be easily accommodated. This configuration allows a large number of photometric and spectroscopic observing modes, and the observer can switch rapidly between different modes in re-

mote operation, for instance, adapting the observations to the seeing conditions of the night.

## 2. Observing modes

The instrument is provided with the following imaging and spectroscopic observing modes:

- wide-field imaging with a plate scale of 0.25''/pixel and a total field, as projected on the sky, of more than 4'  $\times$  4'; wide- and narrow-band filters are available for photometry and in-line imaging;
- small-field imaging with a plate scale of 0.13''/pixel ( $\sim$  2'  $\times$  2' field of view), for better sampling under excellent seeing conditions;
- medium- to low-dispersion long-slit (4' slit) grism spectroscopy with a resolving power between 300 and 1300;
- very low-dispersion long-slit (4' slit) spectroscopy with a resolving power  $\approx$  50, by means of an Amici prism;
- imaging polarimetry for both wide- and small-field imaging mode. Polarimetry imaging is performed on only 1/4 of the field of view, but simultaneously on four directions of polarization angle (0, 45, 90, and 135 degrees), with a clear gain of relative sensitivity.
- spectro-polarimetry with a reduced (25%) slit length, but with four directions of polarization angle (0, 45, 90, and 135 degrees) measured simultaneously.

Send offprint requests to: C. Baffa

<sup>★</sup> Based on observations taken at TNG, La Palma.

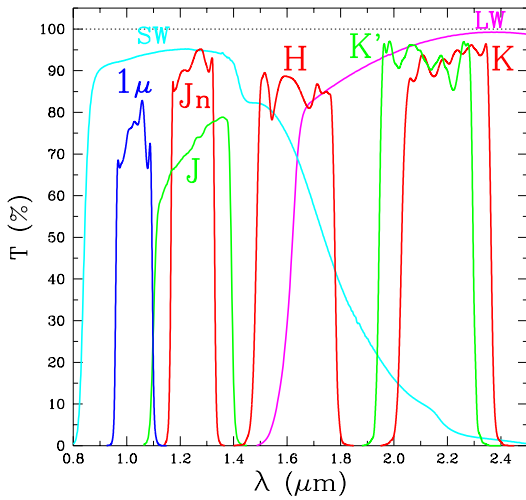


**Fig. 1.** Spectral response and efficiency of NICS wide-band filters.

Three of these modes, low-dispersion long-slit spectroscopy and simultaneous angle polarimetry/spectropolarimetry are unique to NICS, and provide for the first time the possibility to perform reliably these measurements in the infrared.

The simultaneous mode polarimetry is obtained by means of wedged double Wollaston prisms and a special field stop (Oliva 1997). High spatial resolution imaging at the diffraction limit of the telescope is possible by means of an external adaptive optics module (Ragazzoni 1996), using the re-imaging optics of the adaptive module, which has an  $f/33$  output beam. Two reduced plate scales (about  $0.08''$  and  $0.04''$  per pixel, respectively) are available in connection with the wide field and the small-field optics of NICS.

Figure 1 shows the spectral response and the efficiency of the wide band filters which are presently available; besides the standard filters for J, H, and K bands, NICS offers the  $1\mu\text{m}$  filter centered at  $1.030\ \mu\text{m}$  in correspondence with a fair atmospheric window, the  $J_n$  filter as defined by the Gemini project, the  $K'$  filter which cuts the K band portion where the thermal emission dominates the background flux. There is also a band pass filter (labeled SW) for general purpose observations and pointing and a high-pass filter (labeled LW) which, along with the spectral response of the detector, acts as band pass for longer wavelengths.

The narrow-band filter set includes  $\text{Br}\gamma$  and  $\text{Fe II}$  filters, plus the associated K and H narrow-band filters to sample the near-by continuum. It is possible to insert in the beam several accurate grey filters to reduce the flux from very bright sources. Figure 2 shows the resolving power (when associated with the  $1''$  slit) and the efficiency of the available grisms which are resin-replicated Milton-Roy gratings on IRGn6 prisms (Vitali et al., 2000).

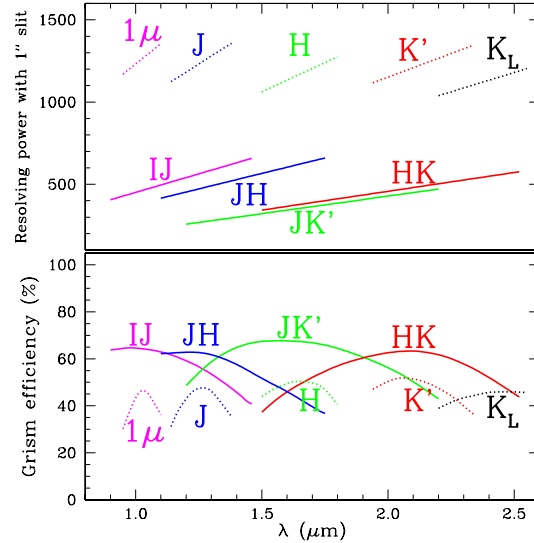


**Fig. 2.** Resolving power and efficiency of NICS grism.

### 3. General Description

The optical scheme comprises the single collimator and the two cameras; all the optical components reside in a vacuum at a temperature of about 80 K, inside a suitable cryostat. The focal plane masks (field stops and slits) are mounted on a wheel. Immediately after the focal plane, a further removable field stop makes possible polarimetric measurements.

The collimator is an achromatic doublet lens, which images the entrance pupil of the TNG and provides a parallel beam at the pupil plane where Lyot stops can be placed. Immediately after the pupil plane, two adjacent wheels carry filters and grisms. Two interchangeable optical systems relay the image of the focal plane on the detector with the desired magnification.

A third optical system images the entrance pupil on the detector, for the purpose of an accurate alignment of the telescope with the instrument pupil, and is not normally used in routine observations. A short discussion can be found in Gennari et al. (1995).

The spectroscopic mode makes use of the wide-field camera by inserting one of the grisms, located on the second filter wheel, into the parallel beam after the pupil.

The rejection of stray and thermal light is left to the TNG baffles in J, H, and  $K'$  bands. At longer wavelengths, where the thermal radiation could prevail, it is possible to insert a cold stop precisely positioned at the pupil image.

The sensitive element of NICS is the Hawaii  $1024 \times 1024$  pixels HgCdTe array detector (Rockwell Science Center). It has a  $18.5\ \mu\text{m}/\text{pixel}$  pitch and is sensitive to radiation at wavelengths between  $\sim 0.90\ \mu\text{m}$  and  $\sim 2.5\ \mu\text{m}$ . Its performance in term of dark current, efficiency, and read noise, is comparable or better than the  $256 \times 256$  NICMOS 3 (e.g. Lisi et al. 1996).

The electronic noise is dominated by the detector and by the first cold amplifier and is  $\sim 25\ e^-$ , if a suitable number of detector resets (more than 32) is performed at each

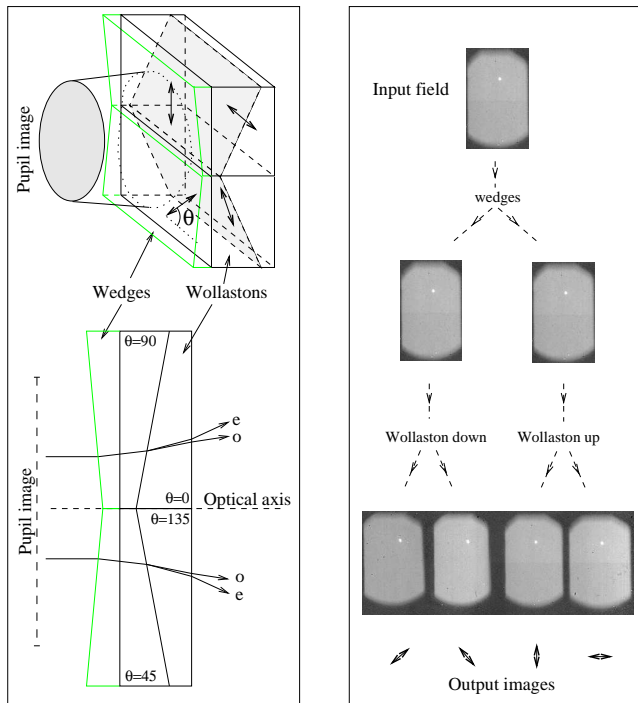


**Fig. 3.** Logical sketch of polarimetry operations. (Adapted from Oliva, 1997, but with real data.)

integration. In the most common read strategy (double sampling), during the integration at least two measurements are performed, one at the beginning (to sample the reset bias level), the second at the end of the integration ramp.

NICS is mounted at the same focal station as the optical CCD camera; the two instruments share an adapter that carries also the adaptive optics module. A plane mirror (M4), mounted on a remotely-operated sliding bench, deflects the beam from the telescope to the entrance of the IR camera, that has its optical axis perpendicular respect to the telescope beam. NICS is mounted on the adapter by means of a set of spherical joints that allows for a limited adjustment of the optical axis alignment respect to the entrance beam. The fine alignment is handled by the M4 mounting hardware, which is designed to allow for small adjustments in matching the telescope optical beam to the camera optical axis.

## 4. Optical Design

The collimator used for all the scales and the observing modes is a detached doublet (BaF<sub>2</sub>-IRG2) (Oliva and Gennari 1998) with spherical-surface lenses that transform the f/11 TNG beam into a 22 mm parallel beam (f/ larger than 2000) with a total level of aberrations below 0.4 mrad. The blur of the entrance pupil image has a maximum size of 0.21 mm at 90% encircled energy, which guarantees an accurate background rejection when the Lyot stop is inserted. The aberrations of the pupil image have been reduced by a factor 2 by means of a mildly

aspheric entrance window, which is designed to leave the pupil plane position unchanged.

The two optical trains for the cameras and the pupil re-imaging system are mounted on a wheel, accurately driven by an external motor. These optics are based on detached doublets (BaF<sub>2</sub>-IRG2) followed by one or two lenses made of the same materials.

The wide-field camera (0.25"/pix) consists of four lenses. The spot blur on the detector is good (90% of the energy within a pixel inside a  $\approx 120''$  radius circle, 75% in the corner). The exit pupil is positioned 88 mm behind the focal plane of the camera, which renders the system not completely telecentric; this introduces some  $\cos^4$  losses (around 4.5% at the corners of the field). In addition, the system suffers a moderate distortion of the order of few percent at the field corners.

The small-field camera (0.13"/pix) consists of three spherical lenses. Its overall image quality is much better than that of the wide-field camera: the spot blur is smaller, distortion is basically absent ( $< 0.16\%$ ), and the exit pupil is at about -350 mm, which makes the system almost telecentric.

The filters are mounted on two wheels located in the parallel beam just after the pupil plane; the second wheel carries also the grisms, slightly tilted with respect to the optical axis to achieve their best efficiency. The second filter wheel also hosts the wedged double Wollaston prism, made of LiYF<sub>4</sub>, that deviates the rays of the parallel beam into four different beams corresponding to the polarization angles of 0, 45, 90 and 135 degrees; as a consequence, the input field of view is split into four images on the detector, one for each of the four polarization angles (Oliva, 1997). This way, one can perform simultaneous photometric measurements of the polarized flux at different angles as required to derive the first three elements of the Stokes vector (see figure 3).

For polarimetry, a suitable field stop right after the focal plane limits the field of view to about 1/4 of the total field, to avoid overlapping of the four polarized images on the detector plane. The second wedged double Wollaston prism is made of LiNbO<sub>3</sub>. This prism is designed to perform spectro-polarimetry when associated with one of the available grisms. The polarizer works with the same principle as the imaging mode, simultaneously delivering four polarized long-slit spectra at angles rotated by 45 degrees. The 4' slit normally used in the spectroscopic mode will be masked to have an equivalent length of about 50'', to avoid any overlapping of the four polarized spectra.

In order to allow focusing capabilities, the detector is mounted on a motorized base. For each optical configuration, the exact detector position has been measured and the control software automatically performs the internal focus setting.

## 5. Cryogenics and Mechanics

The cryo-mechanical design is based on a cylindrical vacuum shell, with a size dictated by the total length of the

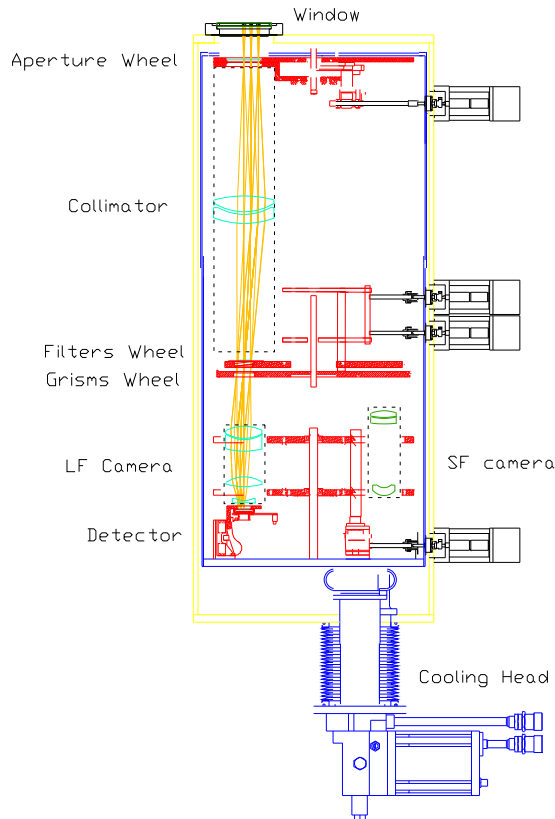


**Fig. 4.** Mechanical Layout of Nics cryostat.

optical system and the wheels diameter. This shape has the advantage of low weight and high stiffness, associated with a reasonable cost.

The cylindrical case, with its symmetry axis orthogonal to the TNG exit beam, is rigidly connected to the Nasmyth adapter flange and supports the internal cooled structure via thermally isolating, rigid elements. The radiation shield is connected to the cold structure; the volume between the pupil plane and the detector is protected from stray light by means of a second radiation shield. The internal structure supports all the optical functions, that is the four wheels (mounted on ball bearings), the collimator, and the detector, keeping them at the required relative positions. Several external micro-stepping motors take care of wheels and slides positioning, as required by the selected observing mode.

Operations at the de-rotated Nasmyth focus necessitate the rotation of the instrument itself, making impractical the use of liquid cryogenics for cooling and maintaining the operative temperature; instead, we based the cryogenic system on a closed cycle cooler.

Because of the relatively large mass of the instrument, cooling it down to the operating temperature is best achieved by means of a continuous flow of liquid nitrogen inside a pipe welded to the optical bench; during normal operation the liquid nitrogen is not necessary. The detector, in good thermal contact with the cold plate, has an

active temperature control. An activated charcoal cryo-adsorption pump is installed on the cold surface to guarantee a good vacuum in the presence of out-gassing or small leaks for periods greater than 90 days. For maintenance purposes, the molecular sieve is equipped with a suitable heating element and thermal switch.

All measurements of temperature and pressure inside the cryostat are transmitted to the control computer, where the software can look after the regularity of operational parameters at scheduled intervals of time.

## 6. Electronics

The data acquisition and control system is based on the controller developed by the CCD Working Group of TNG, suitably modified to adapt it to the architecture of infrared arrays (Comoretto et al. 1995, Comoretto et al. 1999). The controller is based on a set of Transputer processors, which are responsible for handling data and sending commands, and on a DSP Motorola 56001, which generates the synchronized clock pattern needed for accessing and reading the array multiplexer.

The analog signal read on each pixel of the four quadrants is buffered by four FET amplifiers located on the same board that hosts the detector. After that stage, there is a set of four 16-bit A/D converters, which converts the pixel intensity of the four quadrants in parallel. The parallel outputs from the converters are translated to the transputer serial protocol using a dedicated programmable logic chip from Xilinx.

The transputer stage sends the digital data to a Linux PC by means of a fiber link which exploits the fast serial connection capability built into each Transputer. The controller takes care of telemetry and stepper motors by means of dedicated RS-232 serial ports.

## 7. Software

The low-level software involves relatively complex interactions between the Motorola DSP and the cluster of Transputers modules, which operate in a multitasking configuration, each performing an elementary task in parallel. The transputer network is organized as a linear chain with the possibility of single node branches (we call them *left branches*), as described above.

Due to the intrinsic multitasking nature of transputers, we organized low level software as a collection of modules, each performing an elementary task, all acting in parallel. Complex tasks (as data acquisition, handling and transfers) are realized by the cooperation of many modules, often running on different CPUs.

One of the biggest issues we faced in developing transputer software was the inter-processes communication. We developed a simple packet switching solution, in a way that roughly resembles the IP protocol (*Internet way*). All communications are performed by means of fixed-size packets. Each packet starts with a header stating the node of origin, the destination node and destination process,

and the command and sub-command(s). The packet has also a large (1024 short integers) data area.

Each node has a process which examines the header of each packet and then dispatches it to the three possible outward directions or to the destination process for execution. The modified linear chain enables us to make all routing by means of only *local* fast comparisons, which makes the system very efficient and suitable also for data dispatching. For further details on the architecture of the interprocessor communication, see Baffa et al. (1999), Baffa, (2000), and references therein.

The high-level control program, which comprise the telescope interaction, the data handling and storing and the human interface of NICS (Xnics) is based on a similar interface developed several years ago for the Arnica IR camera. Xnics provides the observer with the environment to define the parameters of measurements and to start the desired sequence of integrations (such as single frame, multiple frames, mosaics, scans, scripting language), along with sky-source subtraction and preliminary reduction for quick-look purposes. Several tools are available to control the overall quality of data during the measurement, while the program is in charge of validating the parameters which the observer has chosen before starting the observation. In the background, a task is always active which monitors messages and error flags coming from the low-level software.

All the low level handling is performed by a concurrent program, NICSgate. It consists of several object-oriented processes, each one controlling a special portion of the hardware functionality: telescope, motors, Transnix initialization and programming, acquisition as a defined task and all types of communication in real time. Each process maintains its inner state and can be activated at any time, when an external event needs its special functions.

Due to the intrinsic *network awareness* of both Xnics and NICSgate, a distributed execution of the software is possible: NICSgate on the local acquisition computer, Xnics on a remote one.

The software developed for this instrument is “layer organized”, that is to say organized as a stack of many layers of subroutines of similar levels of complexity. To accomplish its task, each routine needs relies only on the immediately adjacent level and on global utility packages. Such a structure greatly simplifies the development and maintenance of the software.

Our efforts were aimed at several different requirements. Our first priority was to have a flexible laboratory and telescope engine, capable of acquiring easily the large quantity of data a panoramic IR array can produce. Another main goal was to produce an easy-to-use software with the smallest “learning curve”. Our idea was that data acquisition must *disappear* from observer attention, giving him/her the possibility to concentrate on the details of the observations; in this way, observing efficiency is much higher. The human interface is realized through a fast menu interface. The operator is presented only with the options which are currently selectable, and the menu

Filter	J <sub>S</sub>	H	K'
Zero point	22.1	22.3	21.8
Efficiency	0.21	0.28	0.32
Lim. mag.	22.5	21.4	21.2
Average sky mag/arcsec <sup>2</sup>	15.5	13.2	13.2

**Table 1.** Zero points, efficiencies and limiting magnitudes of NICS at the TNG measured in October-December 2000. Lim. Mag. is the point source limiting magnitude for a  $3\sigma$  detection in a hour of on-source integration with a seeing of  $1''$  (integration aperture of  $2''$ ) in LF mode. Average sky is the approximate sky brightness, in magnitudes/arcsec<sup>2</sup> of the various measurements.

is rearranged on the basis of user choices or operations. We have also implemented automatic procedures such as multi-position (“mosaic”), multi-exposure (stack of many frames) and a *scripting language* capable of performing a fairly complex set of measurements with only a “quality control” from the observer.

## 8. Characterization and performance

NICS was tested and characterized both in the laboratory and, at the moment of writing, during four commissioning runs at the TNG.

For what concerns the detector, the current read-out noise (double sampling) is about  $25 e^-$ , but is expected to improve once the forthcoming multi-sampling mode will be available. The dark current is about  $1 e^-/\text{sec}$  and the well capacity is about  $10^5 e^-$ . With the current electronics setup the conversion factor is about  $8 e^-/\text{ADU}$ .

The efficiency of the instrument was measured in the laboratory and at the telescope. In the laboratory,  $2\mu\text{m}$  efficiency was measured by means of a blackbody located in front of the window. The efficiency in imaging mode is about 60%, in agreement with what is expected from the combination of the efficiencies of the detector and of the filters. The overall efficiency of the instrument and telescope (and atmosphere) was measured during the commissioning runs. The total efficiency critically depends on the cleanliness of all optical surfaces, which, for various reasons could be less than perfect. The efficiencies and sensitivities given in the following, refer mostly to the last two commissioning runs, after the cleaning of M3 (the relay mirror to the Nasmyth focus), but without cleaning of the entrance window. The *final* assessment of NICS’ performance at the TNG must await the cleaning of all optical surfaces. In Table 1 we give the zero points in the three main broad bands and the corresponding (total) efficiencies. We report also the limiting magnitudes for a detection at  $3\sigma$  in a hour of on-source integration with a seeing of  $1''$  (integration aperture of  $2''$ ).

The efficiency in the spectroscopic modes agrees with the efficiencies given in Table 1 convolved with the response curves given in Fig. 2. Particularly interesting is

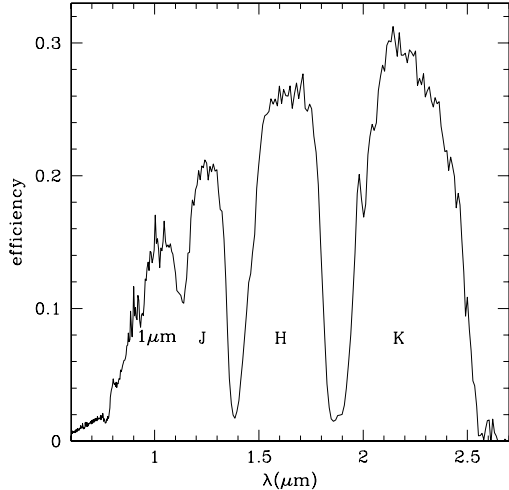


**Fig. 5.** Global efficiency of the system (instrument + telescope + atmosphere) measured through the Amici prism.

Disperser	Central Resolution	Limiting Magnitude
Amici	50	19.8
JK'	350	18.4
IJ	500	18.6
JH	500	18.3
HK	500	18.1
I	1250	17.8
J	1200	17.6
H	1150	17.6
K	1250	17.2

**Table 2.** Limiting magnitudes of NICS at the TNG in different spectroscopic mode. Limiting Magnitude is the point source limiting magnitude for a  $3\sigma$  detection in a hour of on-source integration with a seeing of  $1''$  and with a  $1''$  slit in LF mode, averaged on the wavelength range. The sky luminosity is assumed to be the same as in Table 1.

the efficiency measured through the Amici prism, since the latter disperser has a nearly flat efficiency over the whole near-IR range and, therefore, gives a global view of the efficiency of the system. Fig. 5 gives the (*absolute*) efficiency obtained through the Amici and, more specifically, by dividing the Amici spectrum of a standard star by the intrinsic spectrum of the star (therefore, this is global efficiency of the Amici prism + instrument + telescope + atmosphere). Note the main atmospheric windows which are marked in the figure. Also worth noting is the efficiency drop in the J and  $1\mu\text{m}$  bands which can be ascribed to a drop in efficiency of the detector at short wavelengths.

A broad estimate of the limiting magnitude in polarimetry can be derived from broad-band values by subtracting 1.5 magnitudes (pupil light is divided in four parts). In Table 2 we give preliminary values for spectroscopic limiting magnitudes using large fields, one hour of exposure, and with a  $1''$  slit.

As mentioned in Section 4, the wide-field camera optics suffer from distortion at the level of a few percent at the array vertices. During commissioning, this distortion was characterized at the telescope by measuring crowded stellar fields with known astrometry. It turns out that the distortion can be well approximated by a symmetric radial sixth-order polynomial, and the coefficients for the forward and inverse transformations were derived from astrometric measurements. Results show that, during commissioning, the optical center of the array is within one pixel of the center of symmetry of the distortion, and the amplitude of the measured distortion is consistent with, perhaps slightly smaller than, the design specifications.

## 9. Conclusions

After several months of testing at TNG, NICS proved able to provide the entire set of observing modes included in the design with the desired performance. At present, the TNG is equipped with a near-IR facility well suited to a 3.5m-class telescope, ready to serve the astronomical community.

Two of the available observing modes, polarimetry and low resolution simultaneous  $0.9\text{--}2.5\ \mu\text{m}$  spectroscopy are unique to NICS and make the TNG + NICS system the only facility available for this kind of observations.

*Acknowledgements.* Most of the instrumentation projects for astronomy can be successfully achieved only with the help of a team of skilled engineers and astronomers. The authors would like to emphasize that the NICS project received (and is still receiving) support, help and technical input from several people; they thank in particular A. Marconi, L. Miglietta, G., Tofani, F. Fusi Pecci, L. Corcione, G. Nicolini, J. Licandro, the TNG development team, the CCD Group, and many people from Arcetri and from the astronomical community for useful discussions. The authors would like to particularly acknowledge the support coming from the TNG staff, always ready to help during the difficult and busy time of the commissioning at the telescope.

## References

- Barbieri C., TNG Technical Report n. 53, November 1995
- Baffa C., and Comoretto G., 1996, Arcetri Technical Report N.3/96
- Baffa C., Comoretto G., Gavriushev, V., Giani, E., Lisi F., 1999, *Mem. Soc. Astron. It.* in press
- Baffa C., 2000, Arcetri Technical Report N.2/2000
- Comoretto G., Baffa, C. Gavriushev, V., Giani, E., Lisi F., 1999, *Mem. Soc. Astron. It.* in press
- Comoretto G., Baffa C., and Lisi F., 1995, Arcetri Technical Report N.4/95
- Fusi Pecci F., Stirpe G.M., TNG Instrument Plan, 1992, Osservatorio Astronomico di Bologna.

- Fusi Pecci F., Stirpe G.M., Zitelli V., TNG Instrument Plan:II. A Progress Report, 1994, Osservatorio Astronomico di Bologna.
- Lisi F., Baffa C., Biliotti V., Bonaccini D., Del Vecchio C., Gennari S., Hunt L.K., Marcucci G., Stanga S., 1996, *PASP*, **108**, p364.
- Gennari S., Vanzi, L., Lisi F., 1995, *SPIE*, **2475**, 221.
- Maiolino R., Rieke G.H., Rieke M.J., 1996, *AJ*, **111**, 537
- Oliva E., 1997, *A&AS*, **123**, 589
- Oliva E., Gennari S., 1998, *A&AS*, **128**, 5890
- Oliva E., Origlia L. 1992, *A&A*, **254**, 466
- Ragazzoni R. (ed.), AdOpt Yearly Status Report, 1996, Osservatorio Astronomico di Padova
- Vitali, F., Cianci, E., Lorenzetti, D., Foglietti, V., Notargiacomo, A., Giovine, E., Oliva, E., 2000, *SPIE*, **4008**, 1383.